Synthesis and Thermal Properties of Hybrid Copolymers of Syndiotactic Polystyrene and Polyhedral Oligomeric Silsesquioxane

LEI ZHENG, RAJESWARI M. KASI, RICHARD J. FARRIS, E. BRYAN COUGHLIN

Polymer Science and Engineering Department, University of Massachusetts, Amherst, Massachusetts 01003

Received 25 October 2001; accepted 14 January 2002

ABSTRACT: Copolymerizations of styrene and the polyhedral oligomeric silsesquioxane (POSS)–styryl macromonomer 1-(4-vinylphenyl)-3,5,7,9,11,13,15-heptacyclopentylpentacyclo [9.5.1.1^{3,9}.1^{5,15}.1^{7,13}] octasiloxane have been performed with $CpTiCl_3$ in conjunction with methylaluminoxane. Random copolymers of syndiotactic polystyrene (sPS) and POSS have been formed and fully characterized with ^1H and ^{13}C NMR, gel permeation chromatography, differential scanning calorimetry, and thermogravimetric analysis. NMR data reveal a moderately high syndiotacticity of the polystyrene backbone consistent with this use of $CpTiCl_3$ as a catalyst and POSS loadings as high as 24 wt % and 3.2 mol %. Thermogravimetric analysis of the sPS–POSS copolymers under both nitrogen and air shows improved thermal stability with higher degradation temperatures and char yields, demonstrating that the inclusion of the inorganic POSS nanoparticles makes the organic polymer matrix more thermally robust. The polymerization activity and thermal stability are also compared with those of reported atactic polystyrene–POSS copolymers. © 2002 Wiley Periodicals, Inc. J Polym Sci Part A: Polym Chem 40: 885–891, 2002; DOI 10.1002/pola.10175

Keywords: polyhedral oligomeric silsesquioxane (POSS); syndiotactic polystyrene; POSS copolymer; polyolefin nanocomposites; organic–inorganic hybrid materials

INTRODUCTION

Recently, a great deal of attention has been focused on nanocomposite materials, which typically refer to discontinuous particulate inclusions with one major dimension on a scale of 1–100 nm. These materials have shown novel and often improved mechanical, thermal, electronic, magnetic, and optical properties.[1] Although a two-phase composite may be organic–organic, inorganic–inorganic, or organic–inorganic, the last is more desirable from the standpoint of combined advantageous performance relative to either of the nonhybrid counterparts. Among the many synthetic approaches to obtaining nanocomposites, the use of structurally well-defined inorganic nanoparticles or clusters is becoming an increasingly important strategy.[2] Despite the effort required to establish methods to form covalently or ionically bonded nanoparticles from suitable precursors, this approach has the advantage that it can control and tune the beneficial phenomena associated with nanostructures over a range of length scales. Furthermore, the problem associated with microphase separation in organic–inorganic composites can be alleviated either through the nanoparticles being covalently bound to a polymer backbone or through modification of their surface properties.

In particular, the use of polyhedral oligomeric silsesquioxane (POSS) nanoparticles has been

---

Correspondence to: E. Bryan Coughlin (E-mail: coughlin@mail.pse.umass.edu)

Journal of Polymer Science: Part A: Polymer Chemistry, Vol. 40, 885–891 (2002)

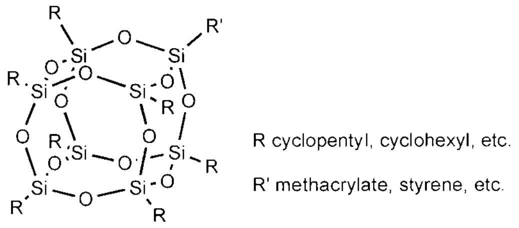

Scheme 1. POSS macromonomer structure.

demonstrated to be an efficient method for designing hybrid nanocomposite materials.[3] A typical POSS nanoparticle contains an inorganic Si_8O_{12} nanostructured skeleton surrounded by eight organic groups labeled R (e.g., isobutyl, cyclopentyl, or cycylohexyl) on the corners to promote solubility in conventional solvents and compatibility with a host polymer matrix. These are generally synthesized through kinetically controlled hydrolytic condensation reactions of $RSiCl_3$ in aqueous acetone. Two predominant stable structures can be obtained: a fully condensed $R_8Si_8O_{12}$ cube and an incompletely condensed $R_7Si_7O_9(OH)_3$ trisilanol.[4–6] POSS macromonomers (Scheme 1) can be prepared from $R_7Si_7O_9(OH)_3$ trisilanol and $R'SiCl_3$ (R′ is a functional group) in a corner-capping reaction.[7] The resulting inorganic core is, therefore, surrounded by seven hydrocarbyl groups and a unique group capable of undergoing polymerization. A variety of functional groups, such as styrene,[7] methacrylate,[8] epoxide,[9] and norbornene,[10] have been prepared. This has afforded the opportunity to incorporate inorganic POSS cages into organic matrices through copolymerizations. This class of organic–inorganic nanocomposites, with nanosize silica covalently bonded to the polymer matrix, is difficult to synthesize otherwise. A variety of POSS-containing copolymers have been prepared with radical techniques, both conventional[7,8] and atom transfer protocols,[11,12] condensation,[13] ring-opening metathesis polymerization,[14] and metallocene catalysis techniques.[15,16] Materials prepared include poly(methyl methacrylate),[8,11,12] polystyrene,[7] epoxy,[9] polysiloxane,[17] polynorbornene,[10] polyethylene, and polypropylene copolymers.[15]

Our current research interests have focused on polyolefin–POSS copolymers. Although these hybrid materials are desirable because of the vast scale of production and wide range of applications for polyolefins, the ability to copolymerize polyolefins with POSS macromonomers with coordination polymerization (Ziegler–Natta or single-site catalysis) is at an early stage of development. Efficient synthetic methods to produce polyethylene–POSS and polypropylene–POSS copolymers have not been reported until recently by our group.[15] In this study, we extend POSS-containing copolymers to syndiotactic polystyrene (sPS). Since the initial report from Ishihara and coworkers,[18,19] sPS has become an attractive engineering thermoplastic because of its high melting temperature (T_m = 270 °C), fast crystallization kinetics, high modulus, and good resistance to water and organic solvents. This work addresses a method to synthesize nanocomposites of sPS and POSS and their resulting thermal properties. The composite matrix of sPS is a semicrystalline material, in contrast to the conventional amorphous atactic polystyrene synthesized by radical polymerization.[7] Different microstructures and, therefore, novel properties are expected because of this crystalline nature.[20]

EXPERIMENTAL

Materials

The cyclopentyl–POSS–styryl macromonomer 1-(4-vinylphenyl)-3,5,7,9,11,13,15-heptacyclopentylpentacyclo $[9.5.1.1^{3,9}.1^{5,15}.1^{7,13}]$ octasiloxane (**1**) was provided by the Air Force Research Laboratory of the Propulsion Directorate at Edwards Air Force Base in California. $CpTiCl_3$ was obtained from Strem. Styrene was obtained from Aldrich and distilled from calcium hydride before use. Methylaluminoxane (MAO) was obtained from Albemarle as a 30 wt % solution in toluene. Toluene was passed sequentially through columns of activated alumina (LaRoche A-2) and Q-5-supported copper redox catalyst (Engelhard CU-0226S) under a prepurified nitrogen atmosphere.[21]

Polymerization Procedures for sPS–POSS Copolymers

The styrene–POSS copolymerizations were carried out in a 100-mL, round-bottom flask equipped with a magnetic stirring bar, 3.12 g (0.03 mol) of styrene, 1.7 mL of a 4.77 M MAO solution (8 mmol), 0.30 g (0.3 mmol; styrene/POSS = 100/1) of POSS–styryl monomer **1**, and toluene. The sealed flask was removed from the

Table 1. Copolymerization of Styrene and POSS–Styryl with $CpTiCl_3$[a]

Sample	[Styrene]/[POSS] (Molar Ratio)	Reaction Time (h)	Yield (g)	POSS[b] wt %	POSS[b] mol %	M_w ($\times 10^3$ g/mol)[c]	PDI[c]	MEK Insolubility (%)[d]
sPS	100/0	0.5	2.23	0	0	33	1.76	90
sPS–POSS-1	100/1	1	1.57	3.3	0.36	37	1.45	89
sPS–POSS-2	100/3	1	1.15	9.9	1.1	35	1.51	~80
sPS–POSS-3	100/5	1	0.90	16	1.9	18	1.50	~60
sPS–POSS-4	100/10	3	0.47	24	3.2	32	1.58	~40

[a] Experimental conditions: 10 μmol of $CpTiCl_3$, 8 mmol of MAO (Al/Ti = 800), 0.03 mol of styrene, and 20 mL of toluene at 50 °C.

[b] As determined by ^{13}C NMR.

[c] Weight-average molecular weight determined with a gel permeation chromatograph coupled to light scattering detectors in 1,2,4-trichlorobenzene at 135 °C.

[d] As calculated from the polymer insoluble in 2-butanone (MEK) after 24 h of Soxhlet extraction.

glove box and heated to 50 °C in an oil bath. A toluene solution of 10 μmol of $CpTiCl_3$ was injected. The total volume of toluene was 20 mL. The polymer was observed to precipitate from the solution during the course of polymerization. After a certain reaction time (see Table 1), polymerization was terminated by the addition of methanol. The copolymers were fully precipitated in 100 mL of a 10% HCl/methanol solution. The copolymer was recovered by filtration, washed with a copious amount of hexanes for the removal of residual **1**, and dried overnight *in vacuo* at 60 °C. The polymerization protocol was repeated with various amounts of **1** (0.3, 0.9, 1.5, or 3.0 g) for the preparation of a range of copolymers. The copolymers were then extracted with refluxing 2-butanone for 24 h in a Soxhlet extractor for the removal of atactic copolymers and possible residual POSS macromonomer.

^1H NMR: 7.0 (br, phenyl-para and ortho positions), 6.5 (br, phenyl-meta position), 1.8 (br, C*H* of the backbone), 1.3 (br, CH_2 of the backbone), 1.6–1.5 (m, CH_2 of cyclopentyl), 1.0–0.9 (m, C*H* of cyclopentyl). ^{13}C NMR (sPS–POSS copolymers): 143.2 (ipso-C of phenyl), 125.9 (phenyl-meta position), 125.6 (phenyl-ortho position), 123.6 (phenyl-para position), 41.5 (*C*H of sPS backbone), 38.4 (CH_2 of backbone), 25.2, 25.1 (CH_2 of cyclopentyl), 20.1 (*C*H of cyclopentyl).

Polymer Characterizations

^1H and ^{13}C NMR spectra were obtained on a Bruker AMX 500 FT NMR spectrometer with tetrachloroethane-d_2 ($CDCl_2CDCl_2$) as the solvent. The residual proton resonance from the solvent at 5.95 ppm was used as the internal reference for ^1H NMR, and hexamethyldisiloxane was used as the reference at 0 ppm for ^{13}C NMR. Quantitative spectra were obtained with a standard inverse-gated proton decoupling pulse sequence and a relaxation delay of 6 s. Gel permeation chromatography was performed with a Polymer Laboratories PL-220 high-temperature gel permeation chromatograph equipped with a Wyatt miniDAWN high-temperature light scattering detector and a refractive-index detector at 135 °C with 1,2,4-trichlorobenzene as a solvent. The miniDAWN detector contained a 690-nm diode laser. A *dn/dc* value of 0.047 mL/g for polystyrene was used. Differential scanning calorimetry was performed on a TA DSC 2910 instrument equipped with a liquid nitrogen cooling accessory unit under a continuous nitrogen purge (50 mL/min). Data reported were gathered for the second melt with a heating and cooling scan of 10 °C/min. Thermogravimetric analysis (TGA) was carried out with a TA instrument TGA 2050 thermogravimetric analyzer at a heating rate of 20 °C/min from room temperature to 700 °C under a continuous nitrogen (100 mL/min) or air (50 mL/min) purge.

RESULTS AND DISCUSSION

Synthesis of sPS–POSS Copolymers

Copolymers of sPS and POSS were synthesized with cyclopentadienyl titanium(IV) trichloride in

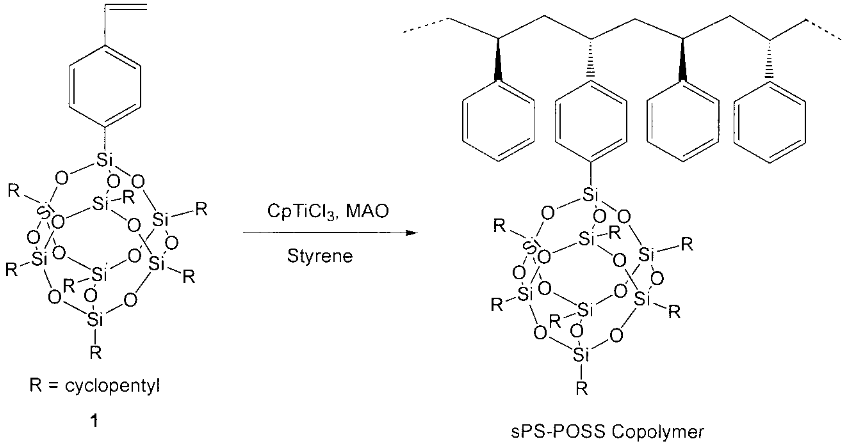

Scheme 2. Copolymerization of styrene and POSS–styryl.

conjunction with MAO (Scheme 2).[18] The reaction conditions, yields, POSS concentrations, and molecular weight data are shown in Table 1. With an increasing POSS concentration, the yields of the copolymers dropped considerably. This observation is in contrast to the trend observed by Haddad and Lichtenhan[7] for the synthesis of atactic poly(4-methyl styrene)–POSS copolymers by a free-radical mechanism; they reported no significant influence on yield. The observed decrease in the yield of the copolymers with the increase in POSS content can be attributed to the coordination polymerization mechanism. The polymers are formed by the coordination of the styrene unit to the cationic titanium metal center, followed by 2,1-insertion of subsequent styrene units in the propagation step.[22] Therefore, in the copolymers, because of the presence of very bulky POSS–styryl units and possible polar interaction between oxygen of the POSS cage and the titanium catalyst center, the propagation rate is much slower than that for styrene. The molecular weights of these copolymers are similar to those of the control homopolymer except for sPS–POSS-3, which decreased from 33 to 18 kg/mol. No significant change, or trend, was observed for the polydispersity indices (PDIs). All were within a range of 1.5–1.8. These polymerizations were all run to moderate levels of conversion for the preservation of random copolymer structures, thereby avoiding the formation of sPS homopolymer. In general, POSS–styryl is less readily incorporated than styrene into the copolymers; an inspection of Table 1 reveals a relative reactivity ratio of approximately 1/300.

Ketones are commonly used to extract atactic polystyrene from a mixture of atactic polystyrene and sPS as a semiquantitative means to measure tacticity. In our case, the Soxhlet extraction of the copolymers was carried out for a day with refluxing 2-butanone as the extraction solvent; this was followed by recovery of the insoluble material. The percentage of insoluble copolymer in refluxing 2-butanone decreased as the POSS content increased. It was first assumed that the increased solubility with an increase in POSS content was due to the decrease in the tacticity of the copolymers. However, ^{13}C NMR of the copolymers proved otherwise (Fig. 1). The carbon peak at 143.2 ppm of the ipso-carbon was used as a reference for the tacticity determination in sPS. For our syndiotactic styrene–POSS copolymers, a single peak at 143.2 ppm was observed for all the copolymers both before and after extraction. This demonstrates that the POSS incorporation does not decrease the tacticity of the copolymers; instead, the loss of crystallinity accounts for the increased solubility (discussed later). ^{13}C NMR also provided information of the extent of the POSS incorporation in the copolymers. As expected, with increasing POSS content in the feed, the extent of the POSS concentration in the copolymers also increased proportionally. The highest concentration obtained in the copolymers was 3.2 mol % (24 wt %).

Thermal Characterization of sPS–POSS Copolymers

The thermal properties of the sPS–POSS copolymers are shown in Table 2. Thermal analysis of

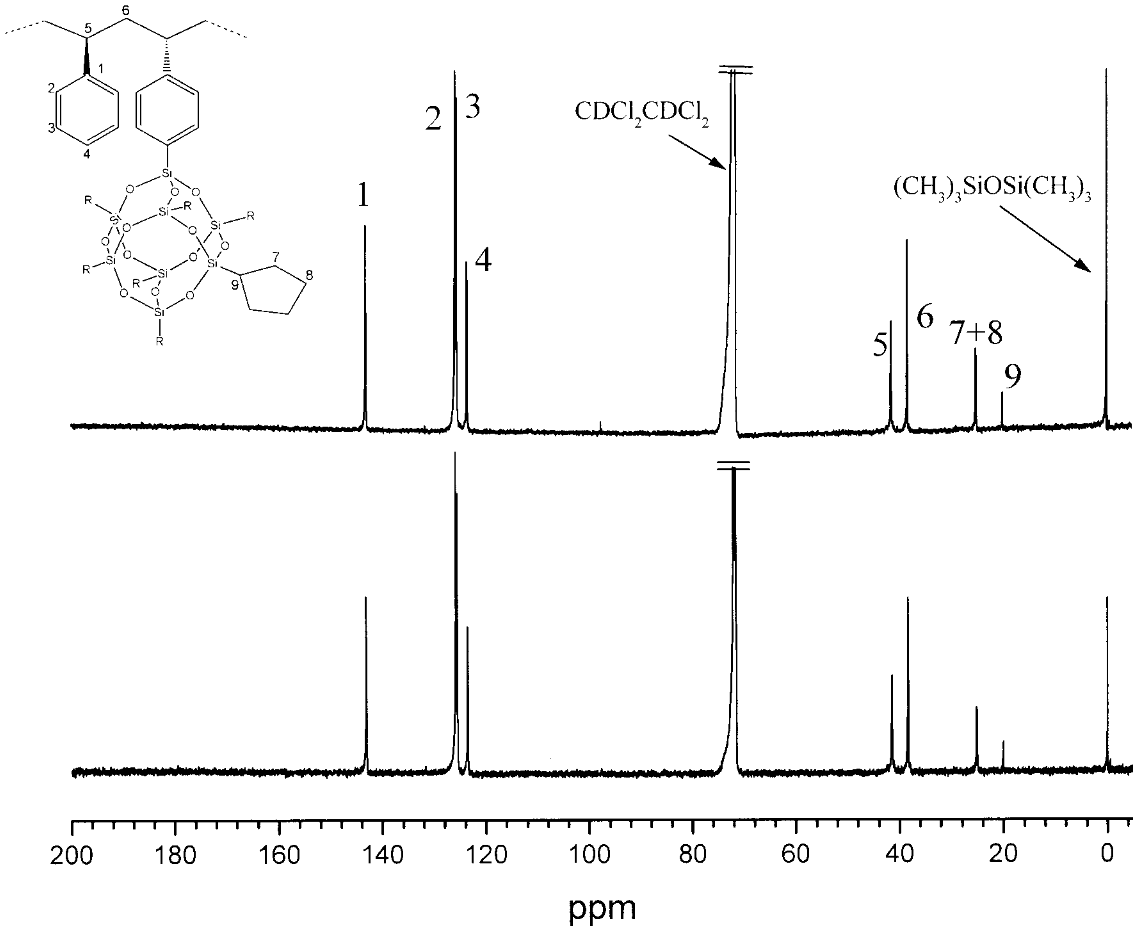

Figure 1. ^{13}C NMR spectra of sPS–POSS-3 (top) before and (bottom) after Soxhlet extraction.

the sPS–POSS copolymers revealed that the glass-transition temperatures (T_g's) of the copolymers had a minor increase from 98 to 102 °C corresponding to 0–3.2 mol % POSS. This is not surprising because Haddad and Lichtenhan[7] reported a dramatic increase in T_g when POSS was increased above 7.8 mol % in atactic poly(4-methyl styrene)–POSS copolymers.[7] We also ob-

Table 2. Summary of the Thermal Characterization of sPS–POSS Copolymers[a]

Sample	T_g (°C)[b]	T_m (°C)[b]	ΔH (J/g)[b]	T_{dec} under N_2 (°C)[c]	Char Yield under N_2 (%)	T_{dec} under Air (°C)[c]	Char Yield under Air (%)
sPS	98	259	28.7	387	0	307	0
sPS–POSS-1	99	255	25.1	398	1.1	307	2.1
sPS–POSS-2	101	245	20.1	394	2.6	300	5.8
sPS–POSS-3	100	237	15.1	397	4.3	321	8.9
sPS–POSS-4	102	—[d]	—[d]	387	17.2	344	21.8

[a] Data were collected for the samples before extraction.
[b] Data were gathered during the second melt with a heating and cooling rate of 10 °C/min.
[c] Temperature at which 5 weight % has been lost, the temperature ramp was 20 °C/min.
[d] Not detectable.

served a melting-point depression of the semicrystalline sPS components upon incorporation of POSS. The melting point of the sPS homopolymer was determined to be 259 °C, whereas T_m of sPS–POSS-3 dropped to 237 °C for 1.9 mol % POSS. The heat of fusion (ΔH) data revealed that the degree of crystallinity also dropped with increasing the POSS content. Interestingly, the sPS–POSS-4 sample with 3.2 mol % POSS did not show a melting peak on the second scan under standard differential scanning calorimetry experimental conditions. Disruption of the crystallization process of sPS due to random incorporation of POSS is attributed to this observation.

Thermal degradation data from TGA demonstrate that the inclusion of the inorganic POSS nanoparticles makes the organic polymer matrix more thermally robust. TGA of the copolymers was performed under both nitrogen and air, and the temperatures of 5% weight loss (T_{dec}) were recorded. T_{dec} recorded from TGA in nitrogen as the carrier gas remained within 387–394 °C. Comparing this set of data to that obtained from Haddad and Lichtenhan,[7] we see that T_{dec} for sPS–POSS copolymers was higher than that obtained for atactic poly(4-methyl styrene)–POSS. Citing specific values and incorporating 1.1 mol % POSS, they observed T_{dec} values of 378–383 °C for 10% weight loss, whereas in our case for the same POSS content, we observed T_{dec} values of 394 °C (5% weight loss) and 402 °C (10% weight loss). This slight increase could arise from the semicrystalline nature of the polymer matrix influencing the aggregation of the inorganic POSS component of the copolymers.[20] The char yield recorded under nitrogen increased considerably from 1.1% for sPS–POSS-1 to 17.2% for sPS–POSS-4. The TGA experiments were also carried out in the presence of air as the carrier gas. T_{dec} remained the same for both sPS and sPS–POSS-1 at 307 °C and then increased with increasing POSS content to 344 °C for sPS–POSS-4, whereas the char yield increased from 2.1% for sPS–POSS-1 loading to 21.8% for sPS–POSS-4. This improvement of thermal oxidative stability is attributed to the formation of a silica layer on the surface of the polymer melt in the presence of oxygen, which serves as a barrier preventing further degradation of the underlying polymer.[23]

CONCLUSIONS

A straightforward synthetic route for preparing sPS–POSS copolymers has been described. Copolymerizations of styrene and POSS–styryl **1** afforded a novel nanocomposite of sPS and POSS. The activity of the copolymerizations is much slower compared with that of radical polymerization, presumably because of the coordination polymerization mechanism. The ^{13}C NMR data reveal a moderately high syndiotacticity of the polystyrene backbone consistent with the $CpTiCl_3$ catalyst used and a POSS loading as high as 24 wt % and 3.2 mol %. TGA of the sPS–POSS copolymers under both nitrogen and air shows improved thermal stability with higher degradation temperatures and char yields.

Financial support was provided by the University of Massachusetts, the National Science Foundation-sponsored Materials Research Science and Engineering Center at the University of Massachusetts, and 3M through a faculty award to E. B. Coughlin.

REFERENCES AND NOTES

1. Nanomaterials: Synthesis, Properties and Applications; Edelstein, A. S.; Cammarata, R. C., Eds.; Institute of Physics: Bristol, 1996.
2. Schubert, U. Chem Mater 2001, 13, 3487–3494.
3. Lichtenhan, J. D. In Polymeric Materials Encyclopedia; Salamone, J. C., Ed.; CRC: Boca Raton, FL, 1996; pp 7768–7777.
4. Brown, J. F.; Vogt, L. H. J Am Chem Soc 1965, 87, 4313–4317.
5. Feher, F. J.; Newman, D. A.; Walzer, J. F. J Am Chem Soc 1989, 1111, 1741–1748.
6. Voronkov, M. G.; Lavrent'yev, V. I. In Topics in Current Chemistry; Boschke, F. L., Ed.; Springer-Verlag: Berlin, 1982; Vol. 102, pp 199–236.
7. Haddad, T. S.; Lichtenhan, J. D. Macromolecules 1996, 29, 7302–7304.
8. Lichtenhan, J. D.; Otonari, Y. A.; Carr, M. J. Macromolecules 1995, 28, 8435–8437.
9. Lee, A.; Lichtenhan, J. D. Macromolecules 1998, 31, 4970–4974.
10. Mather, P. T.; Jeon, H. G.; Romo-Uribe, A.; Haddad, T. S.; Lichtenhan, J. D. Macromolecules 1999, 32, 1194–1203.
11. Pyun, J.; Matyjaszewski, K. Macromolecules 2000, 33, 217–220.
12. Costa, R. O. R.; Vasconcelos, W. L.; Tamaki, R.; Laine, R. M. Macromolecules 2001, 34, 5398–5407.

13. Lichtenhan, J. D.; Vu, N. Q.; Carter, J. A.; Gilman, J. W.; Feher, F. J. Macromolecules 1993, 26, 2141–2142.
14. Zheng, L.; Farris, R. J.; Coughlin, E. B. J Polym Sci Part A: Polym Chem 2001, 39, 2920–2928.
15. Zheng, L.; Farris, R. J.; Coughlin, E. B. Macromolecules 2001, 34, 8034–8039.
16. Tsuchida, A.; Bolln, C.; Sernetz, F. G.; Frey, H.; Mulhaupt, R. Macromolecules 1997, 30, 2818–2824.
17. Shockey, E. G.; Bolf, A. G.; Jones, P. F.; Schwab, J. J.; Chaffee, K. P.; Haddad, T. S.; Lichtenhan, J. D. Appl Organomet Chem 1999, 13, 311–327.
18. Ishihara, N.; Kuramoto, M.; Uoi, M. Macromolecules 1988, 21, 3356–3360.
19. Ishihara, N.; Seimiya, T.; Kuramoto, M.; Uoi, M. Macromolecules 1986, 19, 2464–2465.
20. Zheng, L.; Waddon, A. J.; Farris, R. J.; Coughlin, E. B. Macromolecules, in press.
21. Pangborn, A. B.; Giardello, M. A.; Grubbs, R. H.; Rosen, R. K.; Timmers, F. J. Organometallics 1996, 15, 1518–1520.
22. Po, R.; Cardi, N. Prog Polym Sci 1996, 21, 47–88.
23. Gonzalez, R. I.; Phillips, S. H.; Hoflund, G. B. J Spacecraft Rockets 2000, 37, 463–467.